Communication

Hydrogen Atom Transfer Reactions of Iron–Porphyrin–Imidazole Complexes as Models for Histidine-Ligated Heme Reactivity

Jeffrey J. Warren, and James M. Mayer

J. Am. Chem. Soc., **2008**, 130 (9), 2774-2776 • DOI: 10.1021/ja711057t

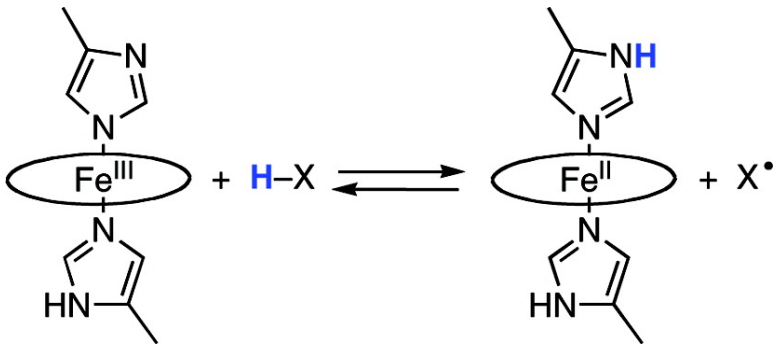

More About This Article

Additional resources and features associated with this article are available within the HTML version:

- Supporting Information
- Links to the 5 articles that cite this article, as of the time of this article download
- Access to high resolution figures
- Links to articles and content related to this article
- Copyright permission to reproduce figures and/or text from this article

View the Full Text HTML

J|A|C|S
COMMUNICATIONS

Published on Web 02/08/2008

Hydrogen Atom Transfer Reactions of Iron−Porphyrin−Imidazole Complexes as Models for Histidine-Ligated Heme Reactivity

Jeffrey J. Warren and James M. Mayer*

University of Washington, Department of Chemistry, Box 351700, Seattle, Washington 98195

Received December 12, 2007; E-mail: mayer@chem.washington.edu

Histidine-ligated hemes are key cofactors in a wide range of biological redox processes. Many of these hemes are thought to serve purely as electron-transfer cofactors; however their pH-dependent redox potentials[1] indicate that they can also react by proton-coupled electron transfer (PCET[2]). Such PCET reactivity has received relatively little attention. The clearest example is perhaps the oxidation of ascorbate by cytochromes b_{561} by a *concerted* proton−electron transfer (CPET) mechanism,[3] as determined by Njus and co-workers using thermochemical considerations.[4] The heme *b* centers in the mitochondrial bc_1 complex are involved in the interconversion of quinones and hydroquinones, which is inherently a PCET process. We report here that model porphyrin−iron−bis(imidazole) complexes react readily by hydrogen atom transfer (HAT). HAT is, in our view,[3,5] a type of CPET reaction in which a proton and an electron are transferred in a single kinetic step from one donor to one acceptor. These porphyrin−imidazole complexes have been developed as structural, spectroscopic, and electron-transfer models for the growing family of bis(histidine)-ligated heme proteins,[6] which includes the cyt b_{561} and heme *b* centers mentioned above.[7]

Our model system uses iron complexes of tetraphenylporphyrin (TPP) and 4-methylimidazole (ImH), following the studies of Valentine et al.[6] They showed that the use of 4-methylimidazole prevents oligomerization of (TPP)Fe-imidazolate complexes. [(TPP)-$Fe^{III}(ImH)_2$]PF_6 (**Fe^{III}ImH**, Scheme 1) was prepared by a modification of their procedure.[6] The new Fe^{II} derivative $(TPP)Fe^{II}(ImH)_2$ **(Fe^{II}ImH)** was synthesized from (TPP)Fe[8] and ImH, and was characterized by ^{1}H NMR and UV−vis spectroscopies and elemental analysis.[9] The deprotonated Fe^{III} and Fe^{II} complexes, $(TPP)Fe(Im)(ImH)^{0/-}$ (**Fe^{III}Im**[6] and **Fe^{II}Im**), were generated in situ from **Fe^{III}ImH** or **Fe^{II}ImH** with the base DBU (1,8-diazabicyclo(5.4.0)-undec-7-ene). These complexes have not been isolated because of weak binding of the second imidazole.[6] Spectroscopic measurements in acetonitrile show that ImH binding to $(TPP)Fe^{III}(Im)$ has K_{eq} = 1300 ± 100 M^{-1}, consistent with previous studies in toluene and THF.[6] All of the measurements below were performed in acetonitrile containing 5 mM ImH, to ensure that only six-coordinate complexes of both Fe^{II} and Fe^{III} were present. Low-spin configurations are indicated for **Fe^{III}ImH** and **Fe^{III}Im** by the Evans method[10] and for **Fe^{II}ImH** based upon its diamagnetic ^{1}H NMR.[9]

The oxidation of ascorbate by cytochromes b_{561} has been modeled by the reaction of **Fe^{III}Im** with the acetonitrile-soluble derivative tetrabutylammonium 5,6-isopropylidene ascorbate (^{n}Bu$_4$N[HAsc]; eq 1).[11] This substrate should have similar reactivity to ascorbate given the distance of the isopropylidene group from the enol functionality.[12] The reaction of ^{n}Bu$_4$N[HAsc] with a solution of **Fe^{III}Im** results in UV−vis and ^{1}H NMR spectral changes consistent with quantitative conversion to **Fe^{II}ImH** (eq 1). This is a net addition of H$^\bullet$ to **Fe^{III}Im**. Stopped-flow kinetic measurements show that the reaction proceeds very rapidly. Using second-order conditions with the lowest practical concentrations (9.0 μM **Fe^{III}Im** + 10.5 μM HAsc$^-$), the reaction is 45% complete within the 2−4 ms mixing time of our instrument. Global analysis of the available spectral data using SpectFit[13] gave good calculated spectra for **Fe^{III}Im** and **Fe^{III}Im** and the rate constant $k_1 = (3.5 \pm 0.9) \times 10^7$ M^{-1} s^{-1}.[9] The deuterated ^{n}Bu$_4$N[DAsc] reacts more slowly under similar conditions, in solutions containing 5 mM 4-methylimidazole-*N*D. Global analysis gives $k_{1D} = (7.5 \pm 0.8) \times 10^6$ M^{-1} s^{-1} and therefore $k_H/k_D = 4.6 \pm 1.3$.

Scheme 1. Thermochemistry of the $(TPP)Fe(ImH)_2$ System in MeCN

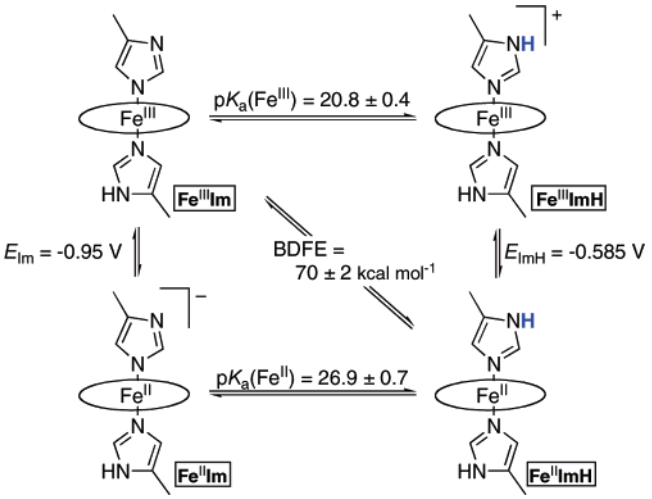

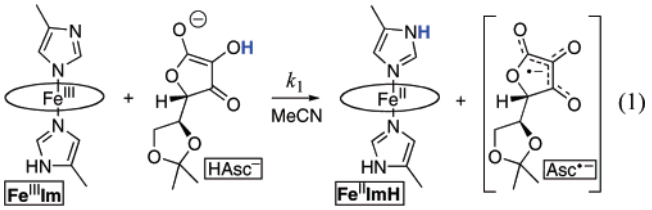

(1)

$k_1 = (3.5 \pm 0.9) \times 10^7$ M^{-1} s^{-1} in MeCN at 298 K

The protonated derivative **Fe^{III}ImH** is also reduced by ^{n}Bu$_4$N[HAsc] to **Fe^{II}ImH**, in a net electron transfer (ET) reaction. Monitoring this reaction by stopped-flow UV−vis spectroscopy shows that it is more than a factor of 10 slower than reaction 1 (Figure S3). The time course can be roughly fit to a second-order rate law (with an apparent *k* of ∼2 × 10^6 M^{-1} s^{-1}) but the kinetics are clearly more complex, especially for the deuterated derivative ^{n}Bu$_4$N[DAsc]. This may be due to rapid reactions of the ascorbyl radical product, HAsc$^\bullet$ or DAsc$^\bullet$, such as protonation of the HAsc$^-$ reactant.[14] DAsc$^-$ reduces **Fe^{III}ImH** more slowly than HAsc$^-$ does (Figure S4), but the kinetic complexity prevents obtaining a value for k_H/k_D.

Electron transfer from HAsc$^-$ to **Fe^{III}ImH** cannot occur by an inner-sphere (coordinated ascorbate) pathway because the exchange

10.1021/ja711057t CCC: $40.75

of bound and free ImH in all these complexes is slow on the ^{1}H NMR time scale. Thus the reduction of **Fe^{III}ImH** likely proceeds via outer-sphere ET from HAsc$^-$. Deprotonated **Fe^{III}Im** has a 0.36 V lower redox potential than **Fe^{III}ImH** (see below), yet is reduced substantially faster under the same conditions. This indicates that the ascorbate reduction of **Fe^{III}Im** proceeds by a mechanism other than outer-sphere ET, most likely by HAT. A HAT path is also indicated by the primary H/D kinetic isotope effect of 4.6 ± 1.3.

Fe^{III}Im reacts rapidly with hydroquinone to give an equilibrium mixture with **Fe^{II}ImH** and benzoquinone (eq 2). This equilibrium

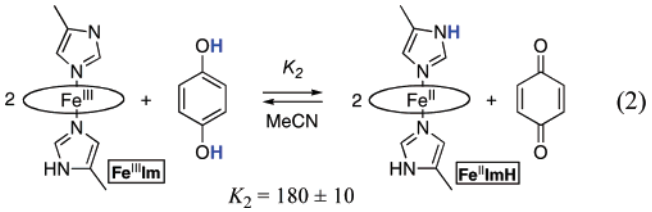

(2)

$K_2 = 180 \pm 10$

can also be established from **Fe^{II}ImH** plus benzoquinone, as observed in both directions by both UV−vis and ^{1}H NMR spectroscopies. Adding aliquots of benzoquinone to **Fe^{II}ImH** and monitoring by optical spectroscopy yields $K_2 = 180 \pm 10$ ($\Delta G°_2 = -3.1 \pm 0.2$ kcal mol^{-1}). These reactions are potential models for quinone/quinol interconversions by the *b* hemes in the bc_1 complex.

Fe^{II}ImH is also rapidly and quantitatively oxidized by the stable phenoxyl radical 2,4,6-^{t}Bu$_3$C$_6$H$_2$O$^\bullet$ to give **Fe^{III}Im** and the phenol (eq 3; by UV−vis and ^{1}H NMR spectroscopies).

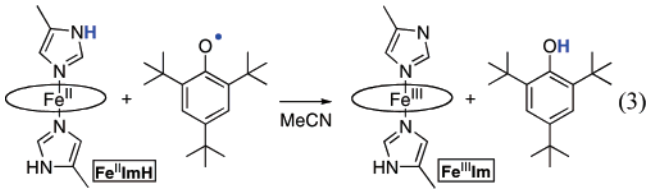

(3)

To probe HAT processes in this system in more detail, the reaction of **Fe^{III}Im** with the hydroxylamine TEMPOH in acetonitrile has been examined. This reaction gives **Fe^{II}ImH** and the nitroxyl radical TEMPO (eq 4), again by net H-atom ($H^+ + e^-$) transfer. The equilibrium constant for reaction 4 was directly measured[9] by optical titration of **Fe^{II}ImH** with TEMPO, in MeCN at 298 K, yielding $K_4 = (4.5 \pm 0.5) \times 10^3$ ($\Delta G°_4 = -5.0 \pm 0.2$ kcal mol^{-1}).

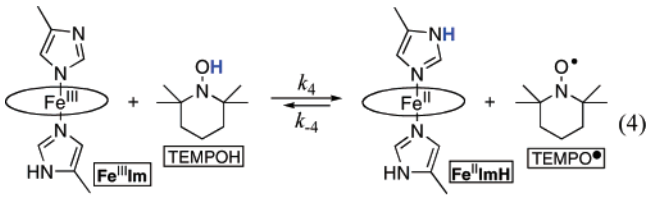

(4)

$k_4 = (9.2 \pm 0.7) \times 10^4$ M^{-1} s^{-1} in MeCN at 298 K

Rate constants for reaction 4 have been determined in MeCN using stopped-flow spectrophotometry (Figure 1).[9] At 298 K, the forward reaction has $k_4 = (9.2 \pm 0.7) \times 10^4$ M^{-1} s^{-1}. k_4 has been measured with 1−16 equiv of TEMPOH, ranging from mixed second-order approach to equilibrium conditions to pseudo-first-order conditions. The reverse reaction between **Fe^{II}ImH** and TEMPO has $k_{-4} = 20 \pm 2$ M^{-1} s^{-1} (measured using a large excess of TEMPO). The ratio $k_4/k_{-4} = (4.6 \pm 0.5) \times 10^3$ is in excellent agreement with the static equilibrium measurements above. Reaction

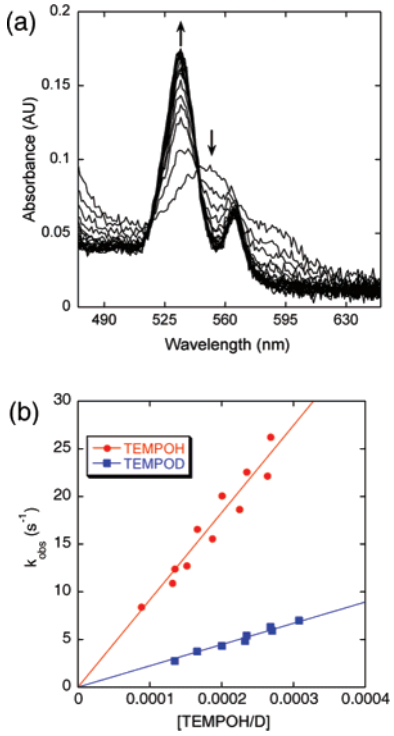

Figure 1. Kinetic data for the reaction of Fe^{III}Im (15 μM) + 150 μM TEMPOH in MeCN (eq 4): (a) visible spectra over 0.3 s; (b) plots of the pseudo-first order k_{obs} vs [TEMPOH/D].

of **Fe^{III}Im** with TEMPO−D proceeds more slowly, with $k_{4D} = (2.2 \pm 0.1) \times 10^4$ M^{-1} s^{-1}; the primary kinetic isotope effect (KIE) is 3.8 ± 0.4.

These reactions can be understood in terms of the thermochemistry of electron, proton, and hydrogen atom transfers in the iron system.[9] Cyclic voltammograms of **Fe^{III}ImH** and **Fe^{II}ImH** show a chemically reversible couple with $E_{ImH} = -0.585 \pm 0.010$ V versus $Cp_2Fe^{0/+}$. Titrations of **Fe^{III}ImH** and **Fe^{II}ImH** with Et_3N ($pK_a = 18.5$ in MeCN[15]) and DBU ($pK_a = 24.3$[15b]), respectively, were monitored by optical spectroscopy to give the pK_a values shown in Scheme 1. The **Fe$^{II/III}$Im** (E_{Im}) redox potential is calculated from these $E°$ and pK_a values, using the edges of Scheme 1 as a closed thermochemical cycle [$RT \ln(K_{FeIII}/K_{FeII}) - F(E_{ImH} - E_{Im}) = 0$]. Finally, eq 5 gives the bond dissociation free energy (BDFE) for an N−H bond in **Fe^{II}ImH** as 70 ± 2 kcal mol^{-1} [C_G(MeCN) = 54.9 kcal mol^{-1} with $E°$ versus $Cp_2Fe^{0/+}$].[16] This value is also independently determined from the equilibrium constants for reactions 2 and 4 given previously. The BDFE of TEMPOH (66.5

$$\text{BDFE[X−H]} = 23.06E° + 1.37pK_a + C_G \text{ (in kcal mol}^{-1}\text{)} \quad (5)$$

± 1 kcal mol^{-1})[17] and $\Delta G°_4 = -5.0 \pm 0.2$ kcal mol^{-1} give BDFE(**Fe^{II}ImH**) as 71.5 ± 1 kcal mol^{-1}. Similarly, $\Delta G°_2 = -3.1 \pm 0.2$ kcal mol^{-1} and the average BDFE for the two hydroquinone O−H bonds (69 ± 2 kcal mol^{-1})[18] gives a **Fe^{II}ImH** BDFE of 70.5 ± 2 kcal mol^{-1}. These values are all in very good agreement.

The equilibrium constant for the TEMPOH reaction (eq 4) has been measured from 276 to 331 K; van't Hoff analysis gives $\Delta H°_4 = -13.0 \pm 1.0$ kcal mol^{-1} and $\Delta S°_4 = -27 \pm 3$ cal K^{-1} mol^{-1}. $\Delta H°_4$ is the difference between the bond dissociation enthalpies (BDEs) of **Fe^{II}ImH** and TEMPOH in MeCN; using BDE(TEMPO−H) = 71.5 ± 1 kcal mol^{-1},[19] the N−H BDE of **Fe^{II}ImH** is 84.5 ± 2 kcal mol^{-1}. The ground-state entropy change for reaction

4 is quite substantial ($T\Delta S°_4 = -8$ kcal mol^{-1}). We have previously reported similarly large $|\Delta S°|$ values for HAT reactions of nonheme iron centers and found them to be an intrinsic property of the $Fe^{III}L/Fe^{II}LH$ redox couple.[16c] The nonzero entropies for these reactions indicate that bond dissociation free energies need to be used for HAT reactions, not the more commonly used BDEs.

The reaction of **Fe^{III}Im** and TEMPOH (eq 4) could in principle occur by initial outer-sphere electron transfer followed by proton transfer (ET/PT), initial PT followed by ET, or by concerted transfer of the electron and proton (HAT/CPET).[3,5] Using the thermochemical data in Scheme 1 and the properties of TEMPOH,[20] the $\Delta G°_{ET}$ for initial electron transfer from TEMPOH to **Fe^{III}Im** to give **Fe^{II}Im** and $TEMPOH^{\bullet+}$ is +38 kcal mol^{-1}. The barrier for initial ET must be at least as large as this value: $\Delta G^{‡}_{ET} \geq \Delta G°_{ET}$. Since this is much larger than the observed Eyring barrier, $\Delta G^{‡}_4 = 10.3 \pm 0.8$ kcal mol^{-1}, ET cannot be the pathway for reaction 4. Similarly, initial PT to give $TEMPO^-$ and **Fe^{III}ImH** has $\Delta G^{‡}_{PT} \geq \Delta G°_{PT} =$ 27 kcal mol^{-1}, again much larger than the observed $\Delta G^{‡}_4$. Thus neither stepwise path can be occurring. Initial HAT, where the proton and electron are transferred in a single kinetic step, is much more favorable ($\Delta G°_4 = -5.0 \pm 0.2$ kcal mol^{-1}) and is the only one of these pathways that is thermodynamically viable. The conclusion that reaction 4 proceeds via a HAT mechanism is supported by the KIE of 3.8.

The ascorbate + **Fe^{III}Im** reaction (eq 1), as noted above, also proceeds by an HAT mechanism. The BDFE for $HAsc^-$ in MeCN has not been reported, but the aqueous BDFE for ascorbate is calculated to be 74 ± 3 kcal mol^{-1} from eq 5, the aqueous thermochemical data,[21] and the aqueous C_G of 57.5 ± 2 kcal mol^{-1}.[16] Our preliminary thermochemical data suggest that the BDFE is lower in MeCN but not lower than the BDFE of TEMPOH. In this light, the 3.5×10^7 M^{-1} s^{-1} rate constant for reaction 1 is rapid, suggesting a small intrinsic barrier to HAT. Ascorbate has been shown to be a competent H-atom donor in both water and acetonitrile,[22] and Njus et al. showed that cyt b_{561} reacts with ascorbate by CPET.[4] Njus did not suggest a deprotonated histidinate ligand analogous to **Fe^{III}Im** but such ligands have been implicated in proton-coupled ET reactions of cyt b_{561}[23] and Rieske proteins,[24] and discussed for other heme cofactors.[25]

In conclusion, the **Fe^{III}Im** and **Fe^{II}ImH** complexes that are models for heme cofactors undergo facile reactions in acetonitrile with an ascorbate derivative, hydroquinone and benzoquinone, phenoxyl and nitroxyl radicals, and a hydroxylamine. These reactions are potential models for biological reactions of histidine-ligated hemes with oxyl radicals and with hydroxyl substrates. The $TEMPO^{\bullet}$/TEMPOH and ascorbate reactions proceed by a hydrogen atom transfer (HAT) pathway, a type of concerted proton−electron transfer (CPET). On the basis of these results, HAT reactions should be considered as part of the primary arsenal of reactivity of histidine-ligated heme cofactors.

Acknowledgment. We gratefully acknowledge support from U.S. National Institutes of Health (GM50422) and the University of Washington.

Supporting Information Available: Experimental details for synthetic, kinetic, and thermochemical studies. This material is available free of charge via the Internet at http://pubs.acs.org.

References

(1) (a) Reid, L. S.; Lim, A. R.; Mauk, A. G. *J. Am. Chem. Soc.* **1986**, *108*, 8197−8201. (b) Reddi, A.; Reedy, C.; Mui, S.; Gibney, B. *Biochemistry* **2007**, *46*, 291−305. (c) Zu, Y.; Fee, J. A.; Hirst, J. *J. Am. Chem. Soc.* **2001**, *123*, 9906−9907. (d) Saraiva, L. M.; Fauque, G.; Besson, S.; Moura, I. *Eur. J. Biochem.* **1994**, *224*, 1011−1017.

(2) (a) Huynh, M. H. V.; Meyer, T. J. *Chem. Rev.* **2007**, *107*, 5004−5064. (b) Cukier, R. I.; Nocera, D. G. *Ann. Rev. Phys. Chem.* **1998**, *49*, 337−369.

(3) Mayer, J. M. *Ann. Rev. Phys. Chem.* **2004**, *55*, 363−390.

(4) (a) Njus, D.; Jalukar, V.; Zu, J.; Kelley, P. M. *Am. J. Clin. Nutr.* **1991**, *54*, 1179S-1183S. (b) Njus, D.; Wigle, M.; Kelley, P. M.; Kipp, B. H.; Schlegel, H. B. *Biochemistry* **2001**, *40*, 11905−11911.

(5) Reference 2a gives a different definition of HAT (p. 5024) that would exclude the reactions described here, because the transferred H^+ forms an N−H σ bond while the e^- formally adds to a different orbital, an iron π-symmetry t_{2g}-type orbital.

(6) Quinn, R.; Nappa, M.; Valentine, J. S. *J. Am. Chem. Soc.* **1982**, *104*, 2588−2595 and references therein.

(7) (a) Shikama, K.; Matsuoka, A. *Crit. Rev. Biochem. Mol.* **2004**, *39*, 217−259. (b) Kundu, S.; Trent, J., III; Hargrove, M. S. *Trends. Plant. Sci.* **2003**, *8*, 387−393. (c) Su, D.; May, J. M.; Koury, M. J.; Asard, H. *J. Biol. Chem.* **2006**, *281*, 39852−39839. (d) Schenkman, J. B.; Jansson, I. *Pharmacol. Therapeut.* **2003**, *97*, 139−152.

(8) Collman, J. P.; Reed, C. A. *J. Am. Chem. Soc.* **1973**, *95*, 2048−2049.

(9) Full details are given in the Supporting Information.

(10) (a) Braun, S.; Kalinowski, H.-O.; Berger, S. *150 and More Basic NMR Experiments* Wiley-VCH: Weinheim, Germany, 1998. (b) Grant, D. H. *J. Chem. Ed.* **1995**, *72*, 39−40.

(11) From 5,6-isopropylidne ascorbic acid (Aldrich) + ^{n}Bu$_4$NOH.[9]

(12) For example: (a) Cabral, J.; Haake, P. *J. Org. Chem.* **1988**, *53*, 5742−5750. (b) Zhang, L.; Lay, P. A. *J. Am. Chem. Soc.* **1996**, *118*, 12624−12637.

(13) Binstead, R. A.; Zuberbühler, A. D.; Jung, B. *Specfit*, version 3.0.38 (32-bit Windows); Spectrum Software Associates: Chapel Hill, NC, 2006.

(14) The protonated radical $HAsc^{\bullet}$ (pK_a of $HAsc^{\bullet}$ is −0.45 in water) is likely to protonate $HAsc^-$ and disproportionate on the timescale of the reaction of **Fe^{III}ImH** + $HAsc^-$. *Ascorbic Acid: Chemistry, Metabolism, and Uses;* Seib, P. A., Tolbert, B. M., Eds.; Advances in Chemistry Series, 200; American Chemical Society: Washington, D.C., 1982 (especially Bielski, B. H. J., pp 81−100).

(15) (a) Isutzu, K. *Acid-Base Dissociation Constants in Dipoloar Aprotic Solvents*; Blackwell Scientific: Oxford, U.K., 1990. (b) Kaljurand, I.; Kütt, A.; Sooväli, L.; Rodima, T.; Mäemets, V.; Leito, I.; Koppel, I. A. *J. Org. Chem.* **2005**, *70*, 1019−1028.

(16) (a) Bordwell, F. G.; Cheng, J.-P.; Harrelson, J. A. *J. Am. Chem. Soc.* **1988**, *110*, 1229−1231. (b) Tilset, M.; Parker, V. D. *J. Am. Chem. Soc.* **1989**, *111*, 6711−6717; **1990**, *112*, 2843. (c) Mader, E. A.; Davidson, E. R.; Mayer, J. M. *J. Am. Chem. Soc.* **2007**, *129*, 5153−5166.

(17) (a) Semmelhack, M. F.; Chou, C. S.; Cortes, D. A. *J. Am. Chem. Soc.* **1983**, *105*, 4492−4494. (b) Mori, Y.; Sakaguchi, Y.; Hayashi, H. *J. Phys. Chem. A* **2000**, *104*, 4896−4905. (c) Bordwell, F. G.; Liu, W.-Z. *J. Am. Chem. Soc.* **1996**, *118*, 10819−10823. (d) Chantooni, M. K., Jr.; Kolthoff, I. M. *J. Phys. Chem.* **1976**, *80*, 1306−1310.

(18) As described in the Supporting Information, the average hydroquinone BDFE was calculated from the known gas-phase thermochemistry[18a,b] and estimates of the free energies of solvation. (a) NIST Chemistry Webbook, http://webbook.nist.gov/chemistry. (b) $S_f°_{(g)}$(benzoquinone): Burcat, A.; Ruscic, B. Third Millennial Ideal Gas and Condensed Phase Thermochemical Database for Combustion with Updates from Active Thermochemical Tables. ftp://ftp.technion.ac.il/pub/supported/aetdd/thermodynamics (accessed 15 July 2007).

(19) (a) Mader, E. A. Ph.D. Thesis, University of Washington, Seattle, WA, 2007. (b) Mader, E. A.; Manner, V. W.; Wu, A.; Mayer, J. M., manuscript in preparation.

(20) $pK_a = 41$ (converted from measurement in DMSO), $E° = 0.71$ V.[9]

(21) Williams, N. H.; Yandell, J. K. *Aust. J. Chem.* **1982**, *35*, 1133−1144.

(22) (a) Bisby, R. H.; Parker, A. W. *J. Am. Chem. Soc.* **1995**, *117*, 5664−5670. (b) Barclay, L. R. C.; Dakin, K. A.; Zahalka, H. A. *Can. J. Chem.* **1992**, *70*, 2148−2153.

(23) Takigami, T.; Takeuchi, F.; Nakagama, M.; Hase, T.; Tsubaki, M. *Biochemistry* **2003**, *42*, 8110−8118.

(24) (a) Zu, Y.; Fee, J. A.; Hirst, J. *J. Am. Chem. Soc.* **2001**, *123*, 9906−9907. (b) Hunsicker-Wang, L. M.; Heine, A.; Chen, Y.; Luna, E. P.; Todaro, T.; Zhang, Y. M.; Williams, P. A.; McRee, D. E.; Hirst, J.; Stout, C. D.; Fee, J. A. *Biochemistry* **2003**, *42*, 7303−7317.

(25) (a) Barker, P. D.; Butler, J. L; de Oliveira, P.; Hill, H. A. O.; Hunt, N. I. *Inorg. Chim. Acta.* **1996**, *252*, 71−77. (b) Arnesano, F.; Banci, L.; Bertini, I.; Ciofi-Baffoni, S.; Woodyear, T. L.; Johnson, C. M.; Barker, P. D. *Biochemistry* **2000**, *39*, 1499−1514. (c) Marques, H. M.; Perry, C. B. *J. Inorg. Biochem.* **1999**, *75*, 281−291. (d) Gattistuzzi, G.; Bellei, M.; Borsari, M.; Di Rocco, G.; Ranieri, A.; Sola, M. *J. Biol. Inorg. Chem.* **2005**, *10*, 643−651.

JA711057T